International Journal of
INTELLIGENT SYSTEMS AND APPLICATIONS IN ENGINEERING
ISSN:2147-6799 www.ijisae.org Original Research Paper

Structural Analysis of Low-Profile Fractal Antennas for Mid-Band Applications

Amrutha R[1] and Gayathri R[2]

Submitted: 25/01/2024 **Revised**: 03/03/2024 **Accepted**: 11/03/2024

Abstract: The mid-band is arguably the most useful band for advanced future technology as it provides an excellent blend of capacity, penetration, speed, and coverage, making it ideal for highly populated urban regions with high connection demand. Fractal antennas with distinct geometric patterns and properties have certain advantages that make them potentially suitable for mid-band applications. In this article, different kinds of low-profile fractal antennas are designed and structurally analyzed for mid-bands, encompassing applications aligned with the IEEE 802.11.4.O Standard. The proposed antennas are assessed through the use of FEM-based simulation software with FR4 as the dielectric material. The proposed Koch fractal stands out as the most promising choice among other antennas for mid-band applications primarily due to its distinctive 15-degree notch characteristic, contributing to its outstanding performance. Experimental testing of the antennas has been conducted, showing favorable agreement with the simulated results.

Keywords: *Fractal, Mid-band, Koch, low-profile, FEM-based.*

1. Introduction

An intriguing area of antenna design research is the integration of fractal concepts with microstrip patch antennas. Microstrip patch antenna performance may be enhanced by fractals, complex geometric structures that display self-replicating patterns at different scales [1]. Antennas with enhanced bandwidth, reduced size, and the ability to function across multiple frequency bands can be produced by applying fractal geometries [2]. The development of imaginative and distinctive antenna designs has been demonstrated to benefit from the application of fractal geometry, such as Koch, Sierpinski Carpet, Minkowski, Sierpinski Gasket, and Hilbert curve [3].

Antennas shaped with Koch fractal pattern function very well at higher frequencies, as showcased in [4]. The goal of this technology is to serve a large number of subscribers with innovative devices. Furthermore, these antennas have low power losses, small geometric dimensions, a wide band characteristic, and generally favorable phase ranges [5].The Sierpinski fractal is predicted to be an effective choice for designing multiband patch antennas [6, 7]. Waclaw Sierpinski first developed this geometry in 1915, and scholars have subsequently experimented with many designs based on it. The Sierpinski fractal is widely recognized for its versatility, since it can be adapted to many shapes such as triangular, rectangular, and circular based on the specific requirements of applications [8].The compactness of the Minkowski fractal design is its primary advantage, as it is crucial for applications like GSM cellular phones [9,10]. The uniform radiation pattern of the Minkowski fractal antenna is similar to that of a standard HWD antenna, which facilitates its easy integration into a variety of wireless communication receivers [11]. Numerous studies suggest that, similar to Koch, Sierpinski carpet, and Minkowski, various types of fractal geometry can be employed to construct a fractal antenna, with each geometry having its own set of advantages and disadvantages [12].

The kind of fractal geometry utilized in fractal patch antenna significantly impacts the antenna's performance in a given application. Therefore, one of the crucial steps in fractal antenna design is determining the appropriate structure that offers the required characteristics for the intended application [13, 14]. This article focuses on identifying suitable fractal geometry for mid-band applications, particularly at 5.2 GHz.

Based on technical considerations, the hypothesis is separated into the following Sections. Section 1 introduces fractal patch antennas, providing insights into their advantages, and includes a literature survey on how fractal geometry contributes to the performance of patch antennas. The comparative simulated outcomes of all low-profile fractal antennas are outlined in Section 3, accompanied by an in-depth examination of the design identified as the most effective. The fourth section provides details on the fabrication process, followed by the measured results of the antennas in the final section. Section 2 primarily focuses on emphasizing the need for a fractal antenna in

[1] *Annamalai University, Chidambaram – 608002, INDIA.*
ORCID ID : 0009-0008-6057-0298
[2] *Annamalai University, Chidambaram – 608002, INDIA*
ORCID ID : 0000-0002-2485-4786
** Corresponding Author Email: amruthaammu27@gmaill.com*

mid-band applications, followed by the design of different types of low-profile fractal antennas suited for mid-band applications. In addition, a complete structural analysis is performed to understand the operation of these antennas and identify the most effective ones among them.

2. Antenna Design:

The present and prospective 5G use cases fall into three categories namely massive machine-type communication (mMTC), ultra-reliable low-latency communication (URLLC) and enhanced mobile broadband (eMBB). Mid-band spectrum is the only type of 5G that is expected to be used for all three of these use cases. Further, it provides more capacity and faster speeds than the low-band, while simultaneously covering a substantially larger area than the high-band millimeter wave spectrum. At this mid-band, there is a considerable demand for an antenna with a high gain and a compact dimension. The optimal choice for achieving this goal is a fractal patch antenna.

The primary objective of this article is to ascertain the fractal geometry that facilitates mid-band applications, especially at the frequency of 5.2 GHz. To achieve this, four different low-profile fractal antennas are constructed and analyzed. The selection of the four antenna structures is based on fundamental waveguide shapes such as square, triangle, and circle. These structures include the Sierpinski carpet, Sierpinski gasket, Koch Island, and Sierpinski circle curve. All four antennas were designed with dimensions of 28 x 45 x 1.6 mm³, utilizing impedance feed. The dimensions of the antenna are calculated by employing the transmission line model, and the equations for the essential parameters [15] are

Effective dielectric constant ϵ_{eff} is given as

$$\epsilon_{eff} = \frac{\epsilon_r+1}{2} + \frac{\epsilon_r-1}{2}\left[1+\frac{12h}{w}\right]^{0.5} \quad (1)$$

Where ϵ_r=dielectric constant; h & w = height and width of the substrate.

Effective length L_{eff} of patch is calculated using

$$L_{eff} = \frac{c}{2f_0\sqrt{\epsilon_{eff}}} \quad (2)$$

Where f_0 = resonant frequency

The variation in length is given by

$$\Delta L = 0.412h\frac{\left(\epsilon_{reff}+0.3\right)\left(\frac{w}{h}+0.264\right)}{\left(\epsilon_{reff}-0.3\right)\left(\frac{w}{h}+0.264\right)} \quad (3)$$

The dielectric material used in these antennas is FR4, which has a dielectric constant of 4.4. The fractal geometry involved in the antenna design is constructed using an Iterated Function System (IFS) based on a deterministic algorithm [16]. An IFS comprises contractions {W_1, W_2, .. , W_N}, where N≥ 2, acting on a closed subset. An attractor of the IFS is a nonempty compact subset F within the closed subset if

$$W(S) = \bigcup_{i=1}^{N} W_i(S) \quad (4)$$

The set {W_1, W_2, ….W_N} represents a collection of affine transformations, U stands for the Hutchinson operator[17], S denotes the initial geometry, and W(S) represents the new geometry generated by applying the set of affine transformations to the original geometry. The affine transformation $W_i(S)$ is precisely defined by the following [18]

$$w\begin{pmatrix}x\\y\end{pmatrix} = \begin{pmatrix}A & B\\C & D\end{pmatrix}\begin{pmatrix}x\\y\end{pmatrix} + \begin{pmatrix}E\\F\end{pmatrix} \quad (5)$$

2.1 Sierpinski Carpet Antenna

The initial design in this section is Sierpinski Carpet antenna with a radiating layer dimension of 20 mm x 14 mm,. A rectangular patch is used in the construction of the Sierpinski carpet fractal. As shown in Fig.1, the appropriate geometry is obtained by subtracting one-third of the rectangle's size from the middle of the main rectangle and repeating the process a number of times. This antenna has undergone two iterations of development [19]. The affine transformation (w_1, w_2 …w_8) that defines IFS of the Sierpinski carpet fractal is given below

$$w_1\begin{pmatrix}x\\y\end{pmatrix} = \begin{pmatrix}1/3 & 0\\0 & 1/3\end{pmatrix}\begin{pmatrix}x\\y\end{pmatrix} + \begin{pmatrix}0\\0\end{pmatrix} \quad (6)$$

$$w_2\begin{pmatrix}x\\y\end{pmatrix} = \begin{pmatrix}1/3 & 0\\0 & 1/3\end{pmatrix}\begin{pmatrix}x\\y\end{pmatrix} + \begin{pmatrix}0\\1/3\end{pmatrix} \quad (7)$$

$$w3\begin{pmatrix}x\\y\end{pmatrix} = \begin{pmatrix}1/3 & 0\\0 & 1/3\end{pmatrix}\begin{pmatrix}x\\y\end{pmatrix} + \begin{pmatrix}0\\2/3\end{pmatrix} \quad (8)$$

$$w_4\begin{pmatrix}x\\y\end{pmatrix} = \begin{pmatrix}1/3 & 0\\0 & 1/3\end{pmatrix}\begin{pmatrix}x\\y\end{pmatrix} + \begin{pmatrix}1/3\\0\end{pmatrix} \quad (9)$$

$$w_5\begin{pmatrix}x\\y\end{pmatrix} = \begin{pmatrix}1/3 & 0\\0 & 1/3\end{pmatrix}\begin{pmatrix}x\\y\end{pmatrix} + \begin{pmatrix}1/3\\2/3\end{pmatrix} \quad (10)$$

$$w_6\begin{pmatrix}x\\y\end{pmatrix} = \begin{pmatrix}1/3 & 0\\0 & 1/3\end{pmatrix}\begin{pmatrix}x\\y\end{pmatrix} + \begin{pmatrix}2/3\\0\end{pmatrix} \quad (11)$$

$$w_7\begin{pmatrix}x\\y\end{pmatrix} = \begin{pmatrix}1/3 & 0\\0 & 1/3\end{pmatrix}\begin{pmatrix}x\\y\end{pmatrix} + \begin{pmatrix}2/3\\1/3\end{pmatrix} \quad (12)$$

$$w_8\begin{pmatrix}x\\y\end{pmatrix} = \begin{pmatrix}1/3 & 0\\0 & 1/3\end{pmatrix}\begin{pmatrix}x\\y\end{pmatrix} + \begin{pmatrix}2/3\\2/3\end{pmatrix} \quad (13)$$

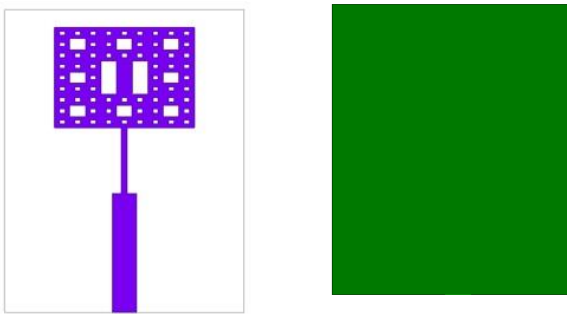

Fig.1. Sierpinski Carpet antenna

In antenna design, the influence of a fractal is often well realized when two parallel capacitances in series with the power line are placed in series with the inductance. In order to accomplish this, an inductance is placed in the mid-void region, as illustrated in Fig.1. With resonance at 5.07 GHz, the findings provide a bandwidth of 170MHz and an efficiency of 52%. The S parameter plot in Fig.5 shows a pure signal with a return loss of -19.29dB. The observed results do not meet the requirements of a mid-band application, as the antenna should ideally offer a return loss of -20 dB. This is because the carpet model has more slots, which causes a stronger capacitive effect within the antenna. Although the structure's impedance feeding will offset the capacitance and provide the device with a steady input, the return loss will still be high .To address this, the antenna structure is modified, and circle design is introduced to meet the required parameters for mid-band application.

2.2 Sierpinski Circle Antenna

In this design, a circular patch is built, with the diameter being the width of the rectangular patch from carpet design. The proper Sierpinski circle geometry [20] is established, as illustrated in Fig.2, by repeatedly deducting one-third of the circle's size from the center of the main circular patch. There have been two development iterations for this antenna.

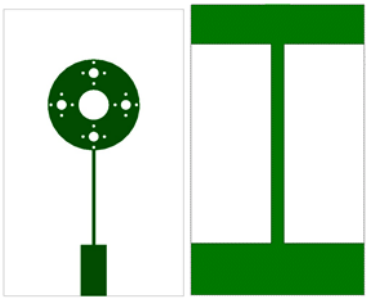

Fig.2. Sierpinski Circle antenna.

The design's variable-length impedance feed line inputs power in to the radiating patch at a high rate, resulting in a gradual signal transmission. This type of design configuration will cover a wider frequency range; nevertheless, the return loss will be high. To enhance the return loss, the ground layer should have a capacitive impact. Therefore, a defected I structure has been incorporated in the ground layer. The antenna is simulated, and its operation is analyzed. The simulation results from Fig.5 indicate that the circle design's resonance is at 5.77 GHz with a bandwidth of 990MHz and a return loss of -30.03 dB. Despite achieving the necessary bandwidth for the mid-band application, the antenna's efficiency is just 54%.The circular capacitance of the radiating layer and the defected ground structure contribute to increased back power radiation, resulting in lower antenna efficiency. Further modifications are made to the antenna configuration, and a triangle design is built in order to satisfy the criteria.

2.3 Sierpinski Gasket Antenna

The construction of the triangle design, the Sierpinski gasket [21, 22], begins with the utilization of an equilateral triangle as its initial geometric element. Using the diameter of the Sierpinski circle from design 2 as its cross angle, the equilateral triangle is constructed. Next, the building process continues with the elimination of the center triangle, whose vertices are situated at the midpoints of the triangle's original sides. To obtain the final structure, as shown in Fig.3, the aforementioned process is repeated for the remaining triangle. This design involves two iterations without any modification to the ground layer. Below is the affine transformation (w1, w2 & w3) that defines the IFS of the Sierpinski gasket fractal

$$w_1\begin{pmatrix} x \\ y \end{pmatrix} = \begin{pmatrix} 1/2 & 0 \\ 0 & 1/2 \end{pmatrix}\begin{pmatrix} x \\ y \end{pmatrix} + \begin{pmatrix} 0 \\ 0 \end{pmatrix} \tag{14}$$

$$w_2\begin{pmatrix} x \\ y \end{pmatrix} = \begin{pmatrix} 1/2 & 0 \\ 0 & 1/2 \end{pmatrix}\begin{pmatrix} x \\ y \end{pmatrix} + \begin{pmatrix} 1/2 \\ 0 \end{pmatrix} \tag{15}$$

$$w_3\begin{pmatrix} x \\ y \end{pmatrix} = \begin{pmatrix} 1/2 & 0 \\ 0 & 1/2 \end{pmatrix}\begin{pmatrix} x \\ y \end{pmatrix} + \begin{pmatrix} 1/4 \\ \sqrt{3}/4 \end{pmatrix} \tag{16}$$

The results obtained from the simulation in Fig.5 demonstrate that the resonance of the gasket design occurs at 5.2 GHz, with a bandwidth of 120 MHz and a return loss of -17.75 dB, respectively. Although the antenna achieves the required resonance for mid-band application, its return loss is significant, and the band coverage is minimal. The capacitive influence of the radiating patch, along with the forward orientation of the triangle's sharp edges, causes this phenomenon to occur. The antenna structure undergoes additional modifications, leading to the construction of Koch design, aimed at achieving the necessary parameters.

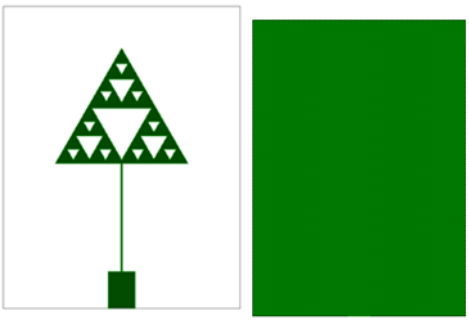

Fig.3. Sierpinski Gasket antenna

2.4 Koch Island Antenna

The Koch Island geometry [23] is designed by dividing the side of the equilateral triangle into three equal parts. Subsequently, the middle segment on each side is replaced with a smaller triangle. The final structure of the Koch antenna, as depicted in Fig.4, is obtained by repeating this process for three iterations. The overall dimension of the radiating patch is kept the same as that of the equilateral triangle in the Sierpinski gasket design. Furthermore, the sharp edges of the Koch Island were constructed with a 15-degree notch to align with the dimensions of the inverted triangle found in the mid-void region of the gasket model. The 15-degree notch construction is implemented to encompass all directions of the design, and this is achieved through the specific manner in which it is constructed. There are six notches in the design; within each notch, there are three sharp edges, each providing 5 degrees. This means that collectively, the notches cover 90 degrees. Additionally, there are six 45-degree gaps between the notches, totalling 270 degrees. By combining the 90 degrees from the notches with the 270 degrees from the gaps between notches, the design incorporates a uniform arrangement of sharp edges that covers the entire 360 degrees of the radiating layer. The Koch Island's IFS is defined by the affine transformations (w1, w2…w7) shown below

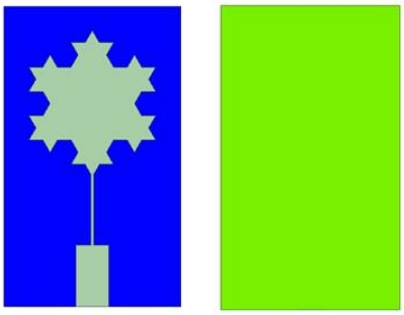

Fig.4. Koch Island antenna

$$w_1\begin{pmatrix}x\\y\end{pmatrix}=\begin{pmatrix}1/2 & -\sqrt{3}/6\\ \sqrt{3}/6 & 1/2\end{pmatrix}\begin{pmatrix}x\\y\end{pmatrix}+\begin{pmatrix}0\\0\end{pmatrix} \quad (17$$

$$w_2\begin{pmatrix}x\\y\end{pmatrix}=\begin{pmatrix}1/3 & 0\\ 0 & 1/3\end{pmatrix}\begin{pmatrix}x\\y\end{pmatrix}+\begin{pmatrix}1/\sqrt{3}\\ 1/3\end{pmatrix} \quad (18)$$

$$w_3\begin{pmatrix}x\\y\end{pmatrix}=\begin{pmatrix}1/3 & 0\\ 0 & 1/3\end{pmatrix}\begin{pmatrix}x\\y\end{pmatrix}+\begin{pmatrix}0\\ 2/3\end{pmatrix}$$

(19)

$$w_4\begin{pmatrix}x\\y\end{pmatrix}=\begin{pmatrix}1/3 & 0\\ 0 & 1/3\end{pmatrix}\begin{pmatrix}x\\y\end{pmatrix}+\begin{pmatrix}-1/\sqrt{3}\\ 1/3\end{pmatrix} \quad (20)$$

$$w_5\begin{pmatrix}x\\y\end{pmatrix}=\begin{pmatrix}1/3 & 0\\ 0 & 1/3\end{pmatrix}\begin{pmatrix}x\\y\end{pmatrix}+\begin{pmatrix}-1/\sqrt{3}\\ -1/3\end{pmatrix} \quad (21)$$

$$w_6\begin{pmatrix}x\\y\end{pmatrix}=\begin{pmatrix}1/3 & 0\\ 0 & 1/3\end{pmatrix}\begin{pmatrix}x\\y\end{pmatrix}+\begin{pmatrix}0\\ -2/3\end{pmatrix} \quad (22)$$

$$w_7\begin{pmatrix}x\\y\end{pmatrix}=\begin{pmatrix}1/3 & 0\\ 0 & 1/3\end{pmatrix}\begin{pmatrix}x\\y\end{pmatrix}+\begin{pmatrix}1/\sqrt{3}\\ -1/3\end{pmatrix} \quad (23)$$

The findings from the simulation presented in Fig.5 show that the Koch design resonates at 5.2 GHz, possessing a bandwidth of 140 MHz and a return loss of -31.45 dB. Furthermore, efficiency is measured at 86%. The Koch design resonates precisely at the desired frequency with minimal return loss, demonstrating superior performance in terms of bandwidth and efficiency for mid-band applications. The 15-degree notch, employed uniformly in a 360-degree fashion throughout the design, distributes power equally in all directions without any harmonics, thereby enhancing the performance of the Koch antenna.

3. Result & Discussions:

In this article, four different types of low-profile fractal antennas designed for mid-band applications are presented, and a comparative analysis is conducted based on their structures. The primary assessment involves evaluating key performance metrics such as bandwidth, return loss, and efficiency. The Koch fractal emerges as the most prominent among the four antennas for mid-band applications, as evidenced by simulated results showcased in Fig.5 and Table.1. Its exact resonance at the desired frequency, coupled with minimum return loss, signifies more effective performance in terms of bandwidth and efficiency. Since the Koch configuration is known to be the most efficient, the results of the following analysis only focus on the Koch island antenna.

Table 1. Basic S-Parameter analysis of different fractals

S: No	Antenna	Resonating Frequency (GHz)	Return Loss (dB)	Bandwidth (MHz)	Gain (dB)	Efficiency (%)
1.	Sierpinski Carpet	5.07	-19.39	170	4.754	52
2.	Sierpinski Circle	5.77	-30.03	990	3.704	54
3.	Sierpinski Gasket	5.2	-17.75	120	2.501	41
4.	**Koch Island**	**5.2**	**-32.84**	**140**	**3.418**	**86**

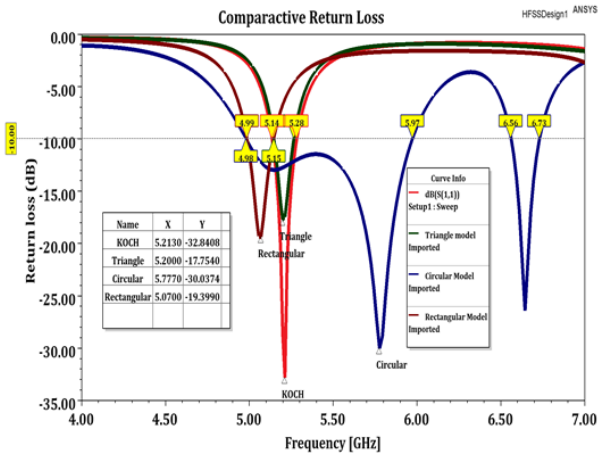

Fig.5. Comparative return loss analysis of different fractals

3.1 VSWR

The evaluation of the Koch Island's performance begins with the analysis of the parameter known as the reflection coefficient. According to transmission line theory, the reflection coefficient, which quantifies the amount of electromagnetic waves reflected due to an impedance mismatch, cannot be directly simulated. Instead, it is determined from the return loss plot. Using the simulated return loss reported in Fig.5, the reflection coefficient of the Koch island antenna is calculated by the following equation [24]:

$$RL = -20\log_{10}\left|\frac{1}{\rho}\right| \tag{24}$$

Where RL= return loss = -32.84 & Reflection co-efficient

$$= \rho \quad \rho = (10)^{-\frac{RL}{20}} = 0.03 \tag{25}$$

Assuming a mismatch in impedance between the antenna and the cable, a portion of the feeding signal is reflected backward. This reflected signal combines with the feeding signal, forming a unified wave referred to as a standing wave. The Voltage Standing Wave Ratio (VSWR) quantifies the ratio between the maximum and minimum values of this standing wave. In an ideal scenario, a VSWR of 1:1 signifies a perfect match, indicating that the impedance of both the antenna and cable are precisely equal. But in real world, the acceptable VSWR is 2:1, which implies that a mismatch with 11% reflected energy is tolerable. The theoretical calculation of VSWR [24] involves the reflection coefficient, and the formula is provided below

$$\rho = \left|\frac{VSWR-1}{VSWR+1}\right| \tag{26}$$

$$VSWR = \frac{\rho+1}{\rho-1} = 1.06 \tag{27}$$

The VSWR obtained through simulation for the Koch Island antenna is depicted in Fig.6. Upon examination, it becomes evident that the manually determined VSWR closely corresponds to the simulated values. The recorded value of 1.05 indicates that the proposed antenna achieves an ideal impedance match at its resonant frequency.

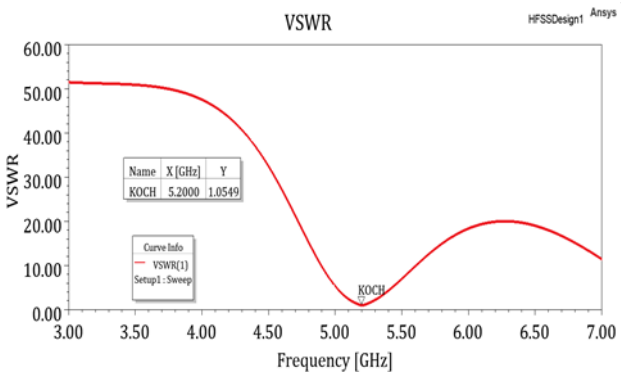

Fig.6. VSWR plot of Koch Island antenna

3.2 Impedance Matching

The polar representation of the complex reflection coefficient is presented in Fig.7. The impedance value identified from the smith chart at resonant frequency is RX=1.0267+0.0691i, where the real part 1.0267 represents resistance value and the imaginary part 0.0691i represents the reactance value. The overall impedance value is determined to be

$|RX| = \sqrt{(1.0267)^2 + (0.069)^2} = 1.028$, implying perfect impedance match, making it compatible with various mid-band devices. The incorporation of 15-degree notches and impedance feed line in the Koch design introduces filtering characteristics, enhancing the impedance matching process. This ensures the acquisition of a pure signal without any deviation in the desired direction.

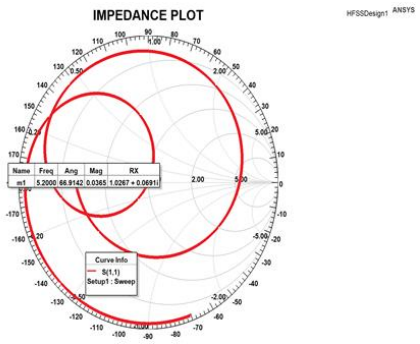

Fig.7. Impedance plot of Koch Island antenna

3.3 Radiation Efficiency

The antenna's efficiency is connected to its gain and directivity. The presence of notches around the circumference of the radiating patch causes the input power to radiate equally in all directions, resulting in the Koch antenna's generated gain being directly proportional to its transmission direction. According to the transmission line property

Gain α Directivity
(28)

In order to remove the proportionality, an effective constant called Efficiency η [24] is added

$$\text{Gain} = \eta \text{ Directivity} \quad (29)$$

$$\eta = \frac{Gain}{Directivity} \quad (30)$$

The gain and directivity of the Koch Island antenna are measured at 3.4158 and 4.0649, respectively, using the 2D plot depicted in Fig.8. Now, the calculated efficiency is found to be

$$\eta = \frac{3.4158}{4.0649} = 84\%$$

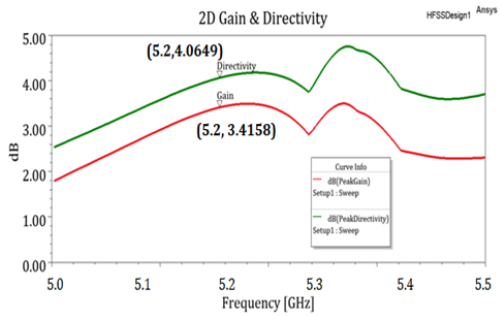

Fig.8. 2D Gain & Directivity plot of Koch Island antenna

The simulated radiation efficiency is depicted in Fig.9. A direct comparison shows a measured efficiency of 86%, indicating a slight deviation from the manually calculated value.

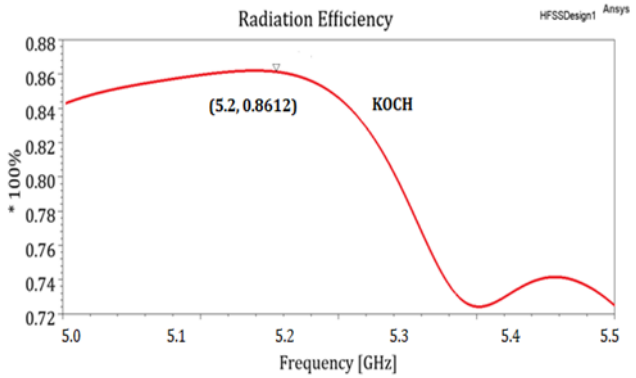

Fig.9. Radiation Efficiency plot of Koch Island antenna

3.4 Radiation Pattern

Generally, in an antenna, if the left-hand circular polarization (LHCP) is equal to the right-hand circular polarization (RHCP), then the antenna is said to exhibit co-polarization, implying that it is circularly polarized. The radiation plot in Fig.10 indicates that the Koch antenna's LHCP equals the RHCP, confirming its circularly polarized behavior. Consequently, the criterion of circular polarization for mid-band applications is met.

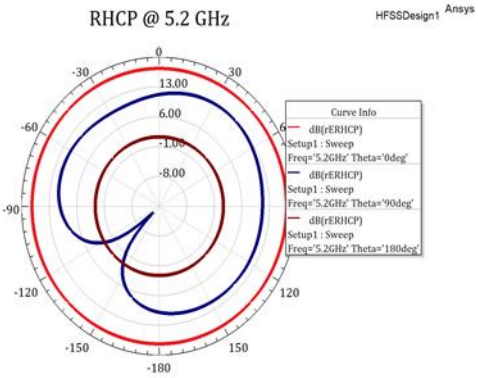

(a)

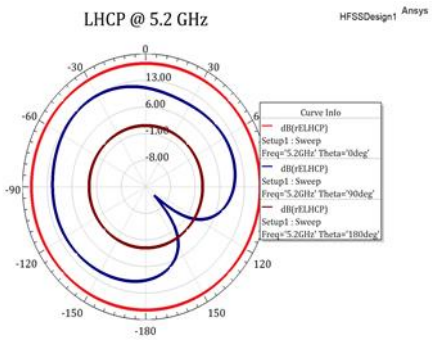

(b)

Fig.10. (a) Right Hand Circular Polarization (b) Left Hand Circular Polarization

4. Fabrication:

The light etching technology was used to construct all four antennas because of its ability to achieve accurate etching

without any noticeable reflections. Fig.11 shows the fabricated antennas.

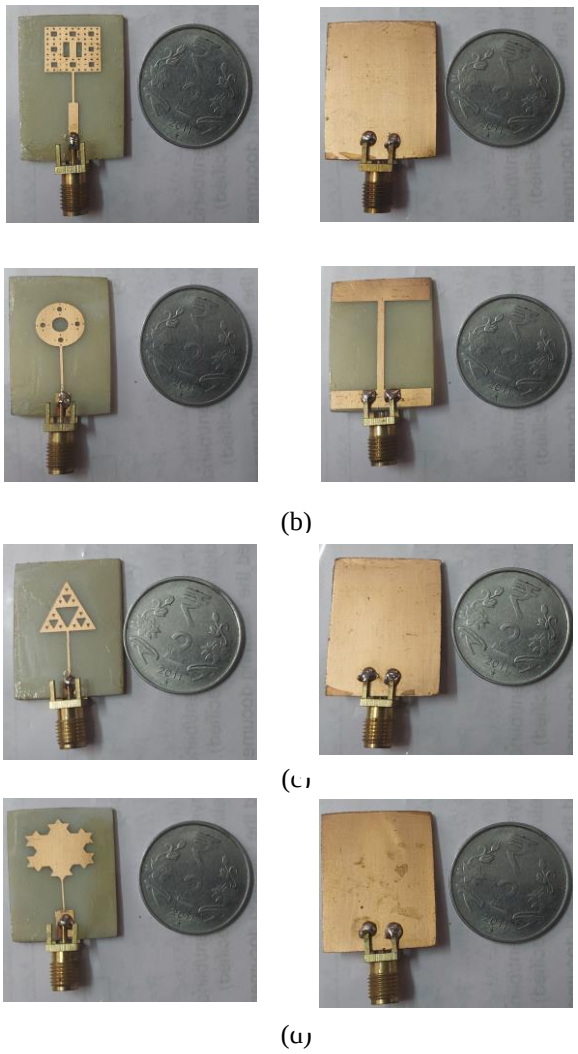

(b)

(c)

(d)

Fig.11. Top & Bottom View of Fabricated antennas (a) Sierpinski Carpet (b) Sierpinski Circle (c) Sierpinski Gasket (b) Koch Island antenna

5. Measured Results:

The measured return loss plots of all four low profile fractal antennas are compared in Fig.12. The finding shows that Koch antenna exhibit superior performance compared to the other three, aligning with the simulated results.

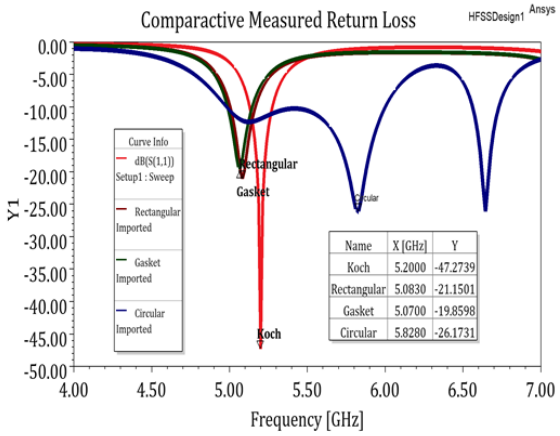

Fig.12. Comparative measured return loss plot

Furthermore, the measured return loss plots of all four low-profile antennas are individually compared with their respective simulated results. From Fig.13, it is apparent that the measured results align with the simulated results with a slight deviation. This discrepancy may be attributed to the antenna fabrication, which is not 100% identical to the simulated dimensions or may involve imperfections in the soldering of the SMA connector.

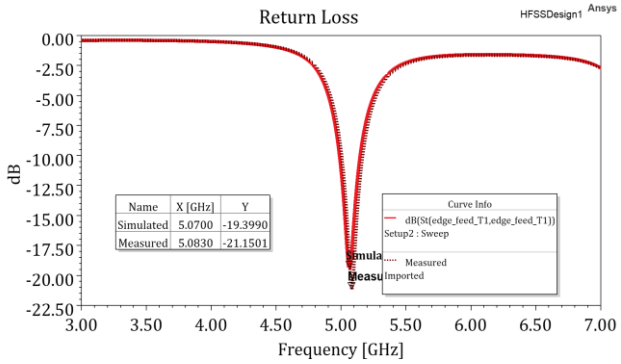

(a)

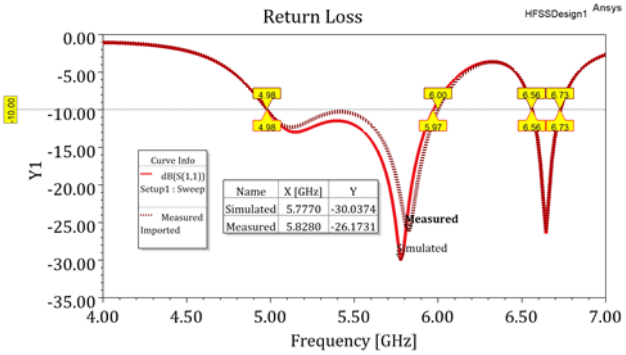

(b)

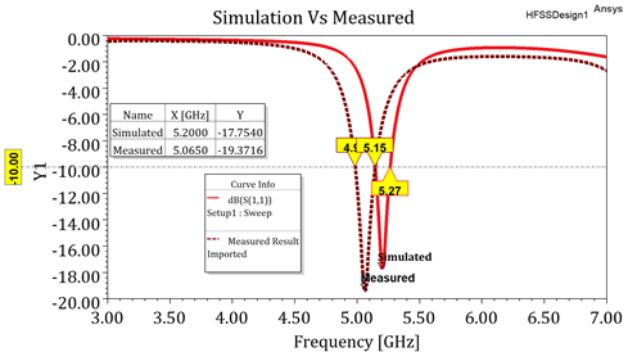

(c)

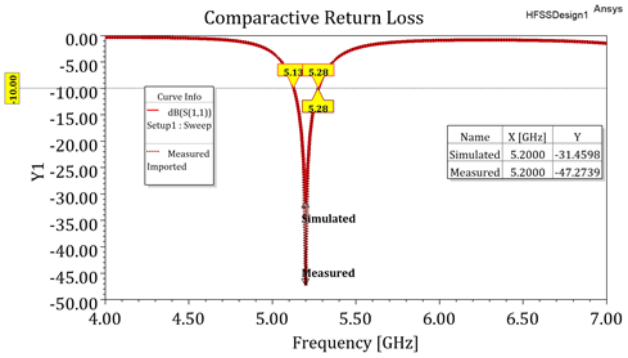

(d)

Fig.13. Measured Vs Simulated return loss plot of (a) Sierpinski Carpet (b) Sierpinski Circle (c) Sierpinski Gasket (b) Koch Island antenna

The comparison between the proposed work and the existing art is provided in Table.2.

Table 2. Comparison with Prior Art

Reference	Fractal Type	Frequency (GHz)	Return loss (dB)	Bandwidth (MHz)	Gain (dB)	Efficiency (%)
[22]	Sierpinski Gasket	5.2	-28.37	-	3.9	-
[25]	Minkowski	5.4	-19.22	185	2.755	56
[26]	Sierpinski Gasket	5	-11.64	390	3.74	65
[27]	Modified Gasket	5.1	-29.38	400	-	-
[28]	Sierpinski Pentagonal	5.2	-20.40	300	3.89	-
Proposed Antenna	**Koch Island**	**5.2**	**-31.45**	**140**	**3.418**	**86**

6. Conclusion

This article conducts a structure-based analysis of various types of low-profile fractal antennas to determine the appropriate fractal geometry for mid-band applications. The comprehensive interpretation of simulated and measured results identifies the Koch fractal as the most suitable candidate. The proposed Koch antenna, with a 15-degree notch characteristic, is found to be compact and offers precise resonance at the required frequency, along with minimal return loss, good gain, and essential circular polarized characteristics. These attributes collectively make it an ideal choice for mid-band applications. In the future, designing the Koch model in an array configuration could enable the acquisition of multiple bands in the mid-band range.

Author contributions

Amrutha R: Study conception, antenna design, material preparation, data collection, analysis and manuscript drafting

Gayathri R: Study conception and Validation

Conflicts of interest

The authors declare no conflicts of interest.

References

[1] D. Froumsia, S. W. Yao, E. D. Jean-Francois, H. Alphonse and M. Inc ," A review of the miniaturization of microstrip patch antenna based on fractal shapes", *Fractals* **30**(5) (2022) 2240161.

[2] Sharma, Narinder, "A Journey of Antenna from Dipole to Fractal: A Review", Journal of Engineering Technology, 2017, 6. 317-351.

[3] Anguera J, Andujar A, Jayasinghe J, Chakravarthy VVSSS, Chowdary PSR, Pijoan JL, Ali T and Cattani C, "Fractal Antennas: An Historical Perspective", *Fractal and Fractional*, 2020; 4(1):3. https://doi.org/10.3390/fractalfract4010003.

[4] Paun, M.-A., Nichita, M.-V., Paun, V.-A., & Paun, V.-P. (2023), "Fifth-generation fractal antenna design based on the Koch Snowflake geometry. A fractal theory application", Expert Systems, e13242. https://doi.org/10.1111/exsy.13242.

[5] Choukiker, Y. K., & Behera, S. K. (2017), Wideband frequency reconfigurable Koch snowflake fractal antenna. IET Microwaves, Antennas and Propagation, 11(2), 203–208.

[6] Narinder sharma and Vipul sharma, "A Novel Hybrid Fractal Antenna for Wireless Application", Progress in electromagnetic Research", Vol 73, May 2018, pp. 25 – 35.

[7] Madhu Sudan Maharana, Guru Prasad Mishra, Biswa Binayak Mangaraj, "Design and simulation of a

Sierpinski carpet fractal antenna for 5G commercial applications", 2017 International Conference on Wireless Communications, Signal Processing and Networking (WiSPNET), pp.1718-1721, 2017.

[8] Guru Prasad Mishra, Madhu Sudan Maharana, Sumon Modak, B.B. Mangaraj, "Study of Sierpinski Fractal Antenna and Its Array with Different Patch Geometries for Short Wave Ka Band Wireless Applications", Procedia Computer Science,Volume 115,2017,Pages 123-134.

[9] Shafie, S. N., Adam, I., & Soh, P. J. (2010). Design and Simulation of a Modified Minkowski Fractal Antenna for Tri-Band Application. 2010 Fourth Asia International Conference on Mathematical/Analytical Modelling and Computer Simulation. doi:10.1109/ams.2010.114

[10] J. P. Gianvittorio, J. P. and Y. Rahmat-Samii, "Fractal antennas: A novel antenna miniaturization technique, and applications," IEEE Antennas Propagation Magazine, Vol. 44, , pp. 20–36, 2002.

[11] M. Ahmed, Abdul-Letif, M.A.Z. Habeeb and H.S. Jaafer, "Performance Characteristics of the Minkowski Curve Fractal Antenna", Journal of Engineering and Applied Sciences, 2006, 1(4), 323-328.

[12] Sharma, Narinder (2017), "A Journey of Antenna from Dipole to Fractal: A Review", Journal of Engineering Technology. 6. 317-351.

[13] Kaliappan and Kavitha, "A Survey on Fractal Antenna Design", International Journal of Pure and Applied Mathematics, Volume 120 No. 6 2018, 10941-10959.

[14] Prakriti Singh, "Application of Fractal Antennas with advantages and disadvantages", International Journal of Creative Research Thoughts, Volume 6, Issue 2 April 2018 , 551-555 , 2320-2882.

[15] Karima Mazen, Ahmed Emran, Ahmed S. Shalaby and Ahmed Yahya, "Design of Multi-band Microstrip Patch Antennas for Mid-band 5G Wireless Communication" International Journal of Advanced Computer Science and Applications(IJACSA), 12(5), 2021. http://dx.doi.org/10.14569/IJACSA.2021.0120557.

[16] J. E. Hutchinson, Indiana University Mathematics Journal 30, pp -713, 1981.

[17] W. J. Krzysztofik, Microwave Review 19, 3 (2013).

[18] Amir pishko, Maslina Darus, Ronak Pashei and Mohammad Sadegh Asgari ,"From Calculating Fractal Dimension to Fabrication of Fractal Antennas" , JCTNS, July 2016.

[19] Aarti Gehani, Prashasti Agnihotri, and Dhaval Pujara, "Analysis and Synthesis of Multiband Sierpinski Carpet Fractal Antenna Using Hybrid Neuro-Fuzzy Model", Progress In Electromagnetics Research Letters, Vol. 68, 59–65, 2017.

[20] Jena, Manas Ranjan, B.B. Mangaraj, and Rajiv Pathak. "Design of a Novel Sierpinski Fractal Antenna Arrays Based on Circular Shapes with Low Side Lobes for 3G Applications." American Journal of Electrical and Electronic Engineering 2, no. 4 (2014): 137-140.

[21] Ramli, M. H., Abd. Aziz, M. Z. A., Othman, M. A., Hassan, N., Noor Azizi, M. S., Azizul Azlan, S. N., … Sulaiman, H. A. (2015), "Design of Sierpinski Gasket Fractal Antenna with slits for Multiband Application", Jurnal Teknologi, 78(5-8). https://doi.org/10.11113/jt.v78.8777.

[22] Sanu, Sanish Vaipel, Stephen Rodrigues, Jisha Krishnan Nair Vallikkunnel, and Sajitha Anpamattathil Sivan. 2023. "Fractal-Enhanced Microstrip Antennas: Miniaturization, Multiband Performance and Cross-Polarization Minimization for Wi-Fi Applications" *Engineering Proceedings* 59, no. 1: 127. https://doi.org/10.3390/engproc2023059127.

[23] Paun, Maria-Alexandra & Nichita, Mihai-Virgil & Paun, Vladimir-Alexandru & Paun, Viorel-Puiu. (2023). Fifth Generation (5G) Fractal Antenna Design Based on the Koch Snowflake Geometry. A Fractal Theory Application. Expert Systems. 10.1111/exsy.13242.

[24] Balanis, C. A. (2005). Antenna theory: Analysis and design (3rd ed.). John Wiley.

[25] Vishnu Prakash, Dr.Jothilakshmi. (2016), "Design And Analysis Of Square Patch Fractal Antenna For C-Band Application", International Journal of Engineering Research & Technology (IJERT) ISSN: 2278-0181.

[26] Ramli, Mohamad & Abd Aziz, Mohamad Zoinol & Othman, Mohd Azlishah & Nornikman, H. & Azizi, Muhammad & Azlan, Siti & Dahalan, Abdul & Sulaiman, Hamzah. (2016). Design of sierpinski gasket fractal antenna with slits for multiband application. Jurnal Teknologi. 78. 123-128. 10.11113/jt.v78.8777.

[27] Ruhika Badhan ,Arushi Bhardwaj and Yogesh Bhomia, "Design of Sierpinski Gasket Antenna for WLAN Applications using Transmission Line Feed", International Journal of Innovative Research in Computer and Communication Engineering, Vol. 4, Issue 8, August 2016.

[28] Ab Rashid, Amier Hafizun, Badrul Hisham Ahmad i Mohamad Zoinol Abidin Abd Aziz. "CPW Fractal Antenna with Third Iteration of Pentagonal Sierpinski Gasket Island for 3.5 GHz WiMAX and 5.2 GHz WLAN Applications." International journal of electrical and computer engineering systems 14, br. 2 (2023): 129-134. https://doi.org/10.32985/ijeces.14.2.2